SRTTU

JCARME
ISSN: 2228-7922
Journal of Computational and Applied Research in Mechanical Engineering
Vol. x, No. x, xxxx
jcarme.sru.ac.ir

Impact of thermal radiation and viscous dissipation on hydromagnetic unsteady flow over an exponentially inclined preamble stretching sheet

S. R. R. Reddy[a] and P. B. A. Reddy[a,*]

[a]Department of Mathematics, S.A.S., Vellore Institute of Technology, Vellore-632014, India.

Article info:

Received: 00/00/2000
Accepted: 00/00/2019
Online: 00/00/2019

Keywords:
Stretching sheet,
Permeability parameter,
Thermal radiation,
Non-uniform heat source or sink,
Chemical reaction.

Abstract

The present numerical attempt deals the sway to transfer of heat and mass characteristics on the time-dependent hydromagnetic boundary layer flow of a viscous fluid over an exponentially inclined preamble stretching. Furthermore, the role of viscous heating, thermal radiation, uneven energy gain or loss, velocity slip, thermal slip and solutal slips are depicted. The prevailing time-dependent PDE's are rehabilitated into coupled non-linear ODE's with the aid of apposite similarity transformations and then revealed numerically by using the 4th order R-K method incorporate with shooting scheme. Influence of various notable parameters like porosity, inertia coefficient, radiation, Eckert number, velocity, thermal and solutal slip are explored via graphs and tables for the cases of assisting and opposing flows. Comparison amid the previously published work and the present numerical outcomes for the limiting cases which are received to be in a righteous agreement. Temperature increments with large values of the non-uniform heat source.

Nomenclature

A	Unsteadiness parameter
A^*	The coefficient of space dependent heat source/sink
B^*	The coefficient of temperature dependent heat source/sink
C	Concentration of the fluid [$kmol\, m^{-3}$]
c_p	Specific heat at constant pressure [$m^2 s^{-2} K^{-1}$]
C_∞	The concentration of the ambient fluid
D	Mass diffusion coefficient [$m^2 s^{-1}$]
Ec	Eckert number
F^*	Dimensional inertia coefficient
F	Dimensionless inertia coefficient
g	The acceleration due to gravity [$m\, s^{-2}$]
Gr	Solutal Grashof number
Gc	Grashof number
K	Permeability parameter
k	Thermal conductivity [$kgms^{-3}K^{-1}$]
k_1	The time-dependent permeability parameter
k^*	The Rosseland mean absorption coefficient
M	Magnetic parameter
M_1	Thermal slip factor
N	Velocity slip factor
Pr	Prandtl number
P	The solutal slip factor
q_r	The radiative heat flux
R	Radiation parameter
Re	Reynolds number
S_f	Velocity slip

*Corresponding author
Email address: pbarmaths@gmail.com

Sc	Schmidt number
S_c	Solutal slip
S_t	Thermal slip
T_∞	The temperature of the ambient fluid [K]
T	Temperature of the fluid [K]
t	The time [s]
u, v	Velocity components in the x and y directions [ms^{-1}]
V_w	The injection/suction velocity

Greek Symbols

δ	Inclination parameter
γ	Chemical reaction parameter
η	Similarity variable
υ	Kinematic viscosity [$m^2 s^{-1}$]
ρ	The density of the fluid [$kg\, m^{-3}$]
β^*	The coefficient of expansion with concentration [$m^2 / kmol$]
σ^*	The Stefan–Boltzmann constant
σ	The electrical conductivity of the fluid
β	The coefficient of thermal expansion [K^{-1}]
ψ	The stream function

Subscripts

∞	Ambient condition
w	Condition at the wall

Superscript

$'$	Differentiation with respect to η

1. Introduction

The boundary layer flow over an extending sheet problem has been actively premeditated for decades because of its extensive applications in technology and industry. Few of these applications are, for example, streamlined expulsion of plastic sheets, hot rolling, MHD generators, accelerators, paper manufacture, artificial fibers, drawing of copper wires, glass blowing, metal turning, drawing plastic films, electronic cooling devices and numerous others. The examination of flow over an extending sheet was pioneered by Crane [1]. Many researchers [2-19] have been scrutinized the various behavior of flow in stretching surfaces. These studies affect with the stretching surfaces where thought to be unfaltering. Few attempts [19–23] have been carried out to describe the unsteady flows in connection with the stretching surfaces. Bachok et al. [24] mentioned the unsteady laminal physical phenomenon flow over a ceaselessly stretching porous surface. The transfer of heat behavior in the unsteady, laminar, incompressible viscous fluid over an extending permeable surface was analyzed by Pal [25]. Misra and Sinha [26] reported the impact of the hydromagnetic flow of blood in porosity in an extensive motion. Srinivas et al. [27] explored the Non-Darcian fluid flow over a permeable extending sheet.

MHD issues occur in a few circumstances like the prediction of room climate, Stream rate estimation and refreshment in nourishment industry. Likewise, MHD is used in geophysics techniques, stellar structures, solar panel, designing MHD pumps, radio communication, interstellar issue etc. Yan Zhang et al. [28] analyzed the thin liquid film flow over an unsteady extending surface in the presence of a variable magnetic field. Hatami et al. [29] studied the unsteady hydromagnetic Couette flows between two parallel infinite plates by utilizing the Differential Transformation Method (analytical method) and Differential Quadrature Method (numerical method). Plasma can be made to collaborate with the magnetic and adjust transfer of heat and erosion trademark. Since few liquids can also emit and absorb thermal radiation, in such circumstance the investigate the influence of magnetic field on the temperature distribution and transfer of heat when the liquid isn't just an electrical conduit yet, in addition, it is equipped for transmitting and engrossing thermal radiation and it has turned into the more prominent significance in space applications. uneven energy gain or loss has a behavior to change the heat dissipation in fluid which consequently affect the molecule statement rate in the framework, for example, semiconductor devices, electronic devices, and atomic pile. Heat source/sink might be viewed as steady, spaceward or heat subordinate. Here, we will examine the space and temperature dependent heat source/sink. Ghadikolaei et al. [30] were investigated unsteady 2D squeezing flow of hydromagnetic fluid between two parallel infinite plates with heat generation/absorption.

Present model exhibits the impact of chemically reacting hydromagnetic flow over an inclined exponentially stretching surface using uneven gain/loss. To the author's consciousness, no

exploration has been done until now in the literature about the influence of slips, viscous dissipation and chemical reaction in an inclined exponentially stretching surface. Such investigations are of awesome significances to engineers and scientists on account of their relatively all-inclusive event in numerous parts of science and engineering. A couple of representative fields of attention in which the transfer of heat and transfer of mass along with chemical reaction in the boundary layer flow has many practical applications in the conveyance of heat and wetness over agribusiness fields and forests of organic product trees, damage of crops because of solidifying, flow in a desert cooler and so on. Enthused by the above studies and the potential applications, a mathematical model is presented here to comprehend the heat and mass characteristics of unsteady hydromagnetic flow of a viscous fluid over an inclined exponentially porous extending surface.

2. Mathematical Formulation

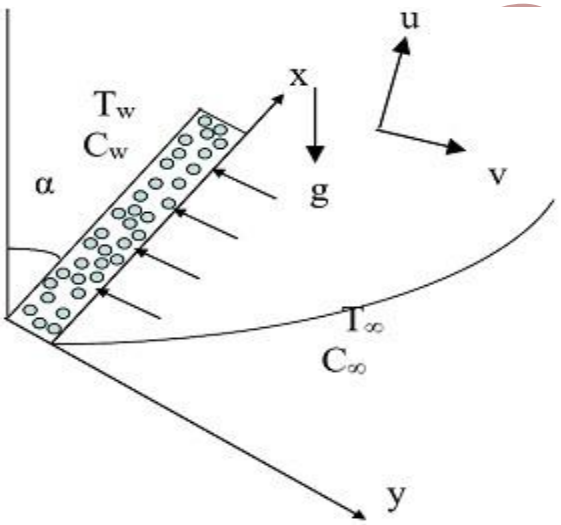

Fig. 1 Physical model of the problem.

Let us consider the two-dimensional(x,y) time dependent hydromagnetic boundary layer flow of a viscous fluid over an exponentially inclined preamble stretching with an acute angle δ to the vertical. Fig. 1 Shows the coordinate system and flow model. At the time $t=0$, the sheet is impulsively stretched with velocity $U_w(x,t)$. A magnetic field *B(t)* is implemented normal to the sheet. The first-order homogeneous time-dependent chemical reaction, solutal, thermal and velocity slip have been taken into account. Then in view of these boundary layer conventions, the continuity, momentum, energy and concentration species can be conveyed as (Magyari and Keller [5], Pal [7], Reddy and Reddy [21] and Chamkha et al. [22]):

$$\frac{\partial u}{\partial x}+\frac{\partial v}{\partial y}=0, \tag{1}$$

$$\frac{\partial u}{\partial t}+u\frac{\partial u}{\partial x}+v\frac{\partial u}{\partial y}=\upsilon\frac{\partial^2 u}{\partial y^2} +\left(\beta\left(T-T_\infty\right)+\beta^*\left(C-C_\infty\right)\right)g\cos\delta -\frac{\sigma B^2}{\rho}u-\frac{\nu}{k_1}u-F^*u^2, \tag{2}$$

$$\frac{\partial T}{\partial t}+u\frac{\partial T}{\partial x}+v\frac{\partial T}{\partial y}=\frac{k}{\rho c_p}\frac{\partial^2 T}{\partial y^2} +\frac{\mu}{\rho c_p}\left(\frac{\partial u}{\partial y}\right)^2-\frac{1}{\rho c_p}\frac{\partial q_r}{\partial y}+\frac{q'''}{\rho c_p}, \tag{3}$$

$$\frac{\partial C}{\partial t}+u\frac{\partial C}{\partial x}+v\frac{\partial C}{\partial y}=D\frac{\partial^2 C}{\partial y^2}-\Gamma\left(C-C_\infty\right). \tag{4}$$

The boundary conditions of aforementioned governing equations are

$$u=U_w+N\mu\frac{\partial u}{\partial y}, v=-V_w, \quad T=T_w+M_1\frac{\partial T}{\partial y}, C=C_w+P\frac{\partial C}{\partial y} \quad \text{at } y=0, \tag{5}$$

$$u\to 0, T\to T_\infty, C\to C_\infty \quad \text{as } y\to\infty.$$

where $V_w, k_1, N, M_1, \Gamma, B, P, U_w, T_w$ and C_w are

$$V_w=f_0\sqrt{\frac{U_0\upsilon}{2L(1-\alpha t)}}e^{\frac{x}{2L}},\ k_1=k_2(1-\alpha t)e^{\frac{-x}{L}},$$

$$N=N_0(1-\alpha t)^{\frac{1}{2}}e^{\frac{-x}{2L}}, M_1=M_0(1-\alpha t)^{\frac{1}{2}}e^{\frac{-x}{2L}},$$

$$\Gamma(t)=\Gamma_0(1-\alpha t)^{-1}e^{\left(\frac{x}{L}\right)}, B=B_0(1-\alpha t)^{-\frac{1}{2}}e^{\left(\frac{x}{2L}\right)},$$

$$P=P_0(1-ct)^{\frac{1}{2}}e^{\frac{-x}{2L}}, U_w=\frac{U_0}{(1-\alpha t)}e^{\frac{x}{L}},$$

$$T_w=T_\infty+\frac{T_0}{1-\alpha t}e^{\frac{x}{2L}}, C_w=C_\infty+\frac{C_0}{1-\alpha t}e^{\frac{x}{2L}}. \tag{6}$$

The non-uniform heat source/sink, q''' is modelled as

$$q''' = \frac{kU_w}{2L\upsilon}\left[A^*(T_w - T_\infty)f' + B^*(T - T_\infty)\right]. \quad (7)$$

The radiative heat flux q_r is given by

$$q_r = -\frac{4\sigma^*}{3k^*}\frac{\partial T^4}{\partial y}. \quad (8)$$

Where k^* and σ^* are the Stefan–Boltzmann constant and Rosseland mean absorption coefficient respectivelly. If the changes of heat discrepancies in the mass of blood flow are trivial. By ignoring higher order terms Eq. (8) can be linearized by expanding T^4 into Taylor's series about T_∞ then we get

$$T^4 \cong 4T_\infty^3 T - 3T_\infty^4. \quad (9)$$

Invoking Eqs. (7), (8) and (9), Equation (3) can be written as

$$\frac{\partial T}{\partial t} + u\frac{\partial T}{\partial x} + v\frac{\partial T}{\partial y} = \left(\frac{k}{\rho c_p} + \frac{16\sigma^* T_\infty^3}{3\rho C_p k^*}\right)\frac{\partial^2 T}{\partial y^2}$$

$$+\frac{kU_w(x,t)}{2L\rho c_p \upsilon}\left[A^*(T_w - T_\infty)f' + B^*(T - T_\infty)\right] \quad (10)$$

$$+\frac{\mu}{\rho c_p}\left(\frac{\partial u}{\partial y}\right)^2$$

We introduce the non-dimensional parameters as

$$\eta = \left(\frac{U_0}{2\upsilon L(1-\alpha t)}\right)^{\frac{1}{2}} e^{\frac{x}{2L}} y, \psi = \left(\frac{2U_0\upsilon L}{(1-\alpha t)}\right)^{\frac{1}{2}} e^{\frac{x}{2L}} f(\eta),$$

$$T = T_\infty + \frac{T_0}{1-\alpha t}e^{\frac{x}{2L}}\theta(\eta),\ C = C_\infty + \frac{C_0}{1-\alpha t}e^{\frac{x}{2L}}\varphi(\eta). \quad (11)$$

Now, introduce ψ function which is expressed as $u = \frac{\partial \psi}{\partial y}$, $v = -\frac{\partial \psi}{\partial x}$, (12)

Now substituting (11) and (12) into the Eqs. (2), (4) and (10), we get

$$f''' - 2(f')^2 + ff'' - (\eta f' + 2f)A$$

$$+(Gr\,\theta + Gc\,\phi)\cos\delta - (M + K)f' \quad (13)$$

$$-F(f')^2 = 0,$$

$$\left(1 + \frac{4}{3}R\right)\theta'' - \Pr(f'\theta - f\theta') - \Pr A(\eta\theta' + 2\theta)$$

$$+Ec\Pr(f'')^2 + B^*\theta + A^* f' = 0, \quad (14)$$

$$\frac{1}{Sc}\phi'' + f\phi' - f'\phi - A(2\phi + \eta\phi') - \gamma\phi = 0. \quad (15)$$

with dimensionless the boundary conditions

$$\left.\begin{aligned} f = f_0,\ f' = 1 + S_f f''(0), \\ \theta = 1 + S_t\theta'(0), \phi = 1 + S_c\phi'(0) \end{aligned}\right\} \text{at}\ \eta = 0, \quad (16)$$

$$f' \to 0, \theta \to 0, \phi \to 0 \qquad as\ \eta \to \infty.$$

where the non-dimensional parameters are given by

$$Gr = \frac{2g\beta L(T_w - T_\infty)}{U_w^2}, Gc = \frac{2g\beta^* L(C_w - C_\infty)}{U_w^2},$$

$$A = \frac{\alpha L}{U_w(1-\alpha t)},\ M = \frac{2L\sigma B_0^2}{\rho U_0}, F = 2F^* L,$$

$$K = \frac{2\upsilon L}{k_2 U_0},\ R = \frac{4\sigma^* T_\infty^3}{kk^*}, Ec = \frac{U_w^2}{(T_w - T_\infty)c_p}, \quad (17)$$

$$\Pr = \frac{\mu c_p}{k}, Sc = \frac{\nu}{D} \text{ and } \gamma = \frac{2L\Gamma_0}{U_0}.$$

Gc solutal Grashof number, *Gr* is the Grashof number, A is the unsteadiness parameter, *M* is the magnetic parameter, *F* is the dimensionless inertia coefficient, *K* is the permeability parameter, *R* is the radiation parameter, *Ec* Eckert number, *Pr* is the Prandtl number, γ is the chemical reaction parameter. *Sc* is the Schmidt number and δ is the inclination parameter.

In Eq. (16), $f_0 < 0$ correspond to injection and $f_0 > 0$ correspond to suction. The solutal slip S_c thermal slip S_t and velocity slip S_f, are as

$$S_f = N_0\rho\sqrt{\frac{\upsilon U_0}{2L}}, S_t = M_0\sqrt{\frac{U_0}{2\upsilon L}} \text{ and}$$

$$S_c = P_0\sqrt{\frac{U_0}{2\upsilon L}}. \quad (18)$$

In the equations written above, primes denote derivatives with respect to η.

The dimensionless skin friction factor (C_f), rate of heat transfer (Nu_x) and rate of mass transfer (Sh_x) which are defined as

$$C_f = \frac{2\mu\left(\frac{\partial u}{\partial y}\right)_{y=0}}{\rho U_w^2} = \sqrt{2}\,\mathrm{Re}_x^{-\frac{1}{2}} f''(0), \quad (19)$$

$$Nu_x = -\frac{x\left(\frac{\partial T}{\partial y}\right)_{y=0}}{(T_w - T_\infty)} = -\mathrm{Re}_x^{\frac{1}{2}}\theta'(0), \quad (20)$$

$$Sh_x = \frac{x\left(\frac{\partial C}{\partial y}\right)_{y=0}}{(C_w - C_\infty)} = -\mathrm{Re}_x^{\frac{1}{2}}\varphi'(0). \quad (21)$$

where $\mathrm{Re}_x = \frac{LU_w}{\upsilon}$ is the local Reynolds numbe

3. Results and discussion

The non-remittal values of the various parameters which we measured as M = 1.0, Gr = 2.0, Gc = 2.0, A = 1.0, $\delta = \frac{\pi}{4}$, F = 0.5, K = 2.0, A^* =-0.5, R = 0.5, B^* = -0.5, Pr = 0.72, Ec = 0.5, Sc = 0.60, f_0 = 0.5, $\gamma = 0.5$, $S_f = 0.5$, $S_t = 0.5$ and $S_c = 0.5$ unless otherwise stated.

The Velocity(f'), temperature (θ) and concentration (ϕ) for numerous values of parameters M, A, K, Gr, Gc, δ, F, S_f, R, A^*, B^*, Ec, S_c, Pr, Sc, γ, f_0 and S_t are portrayed in Figs. 2-6. Fig. 2(a) elucidate that the velocity diminutions with the higher values of M for the cases of opposing, assisting and time-dependent. It is noted that the larger value of M significantly enhances due to Lorentz force. The differences in the f' for variations in the Gc are displayed in Fig. 2(b). From this figure, it very well may be construed that an expansion in the Gc upgrades the speed for opposing, assisting and steady-state cases. Fig. 2(c) depicts the disparity of velocity distribution for various estimations of S_f. It is perceived that the velocity of the boundary layer declines with elevating S_f [21]. The impact of the permeability parameter on the f' is displayed in Fig. 2(d). It tends to be seen that an expansion in the permeability parameter improves the speed. Fig. 2(e) presentations the difference of f' with various values of dimensionless inertia coefficient. Results expose that the f' diminish with a rise in the dimensionless inertia coefficient. The dimensionless velocity transferences for various estimations of the inclination parameter are shown in Fig. 2(f). Results show that the velocity diminishes with the expanding inclination parameter for unsteady and steady-state cases.

Figs. 3(a)-(f) shows the temperature distribution for different estimations of thermal radiation, Eckert number, thermal slip, Prandtl number and heat generation/absorption. The characteristic of R on temperature profile is portrayed in Fig. 3(a) for three different cases. From this, it very well may be deduced that the fluid temperature is enhances by rise the radiation parameter. Fig. 3(b) is planned to reveal insight into the impact of Eckert number on the fluid temperature. It is found that the higher values of Eckert number lead to enhance the fluid temperature. It is revealed that thermal energy is saved in the fluid by frictional heating. It is due to the reason that the larger value of the Eckert numbers is raising the temperature at each point in the fluid. Fig. 3(c) portrays thermal slip impacts on temperature profile for three cases. In this, it tends to be seen that the temperature-related boundary layer thickness lessens with expanding values of velocity slip parameter.

Table 1. The variation of $-\theta'(0)$ for some reduced cases when $\gamma = 0$, M = A = Da = Gr = Gc = Ec = Sc = S_f = S_t = 0 = S_c = 0.

	Bidin and Nazar [2]		Nadeem et al. [3]		Mukhopadhyay and Reddy [4]		Present	
R / Pr	0.5	1	0.5	1	0.5	1	0.5	1
1	0.6765	0.5315	0.680	0.534	0.6765	0.5315	0.67657	0.53155
2	1.0735	0.8627	1.073	0.863	1.0734	0.8626	1.07352	0.86277
3	1.3807	1.1214	1.381	1.121	1.3807	1.1213	1.38075	1.12143

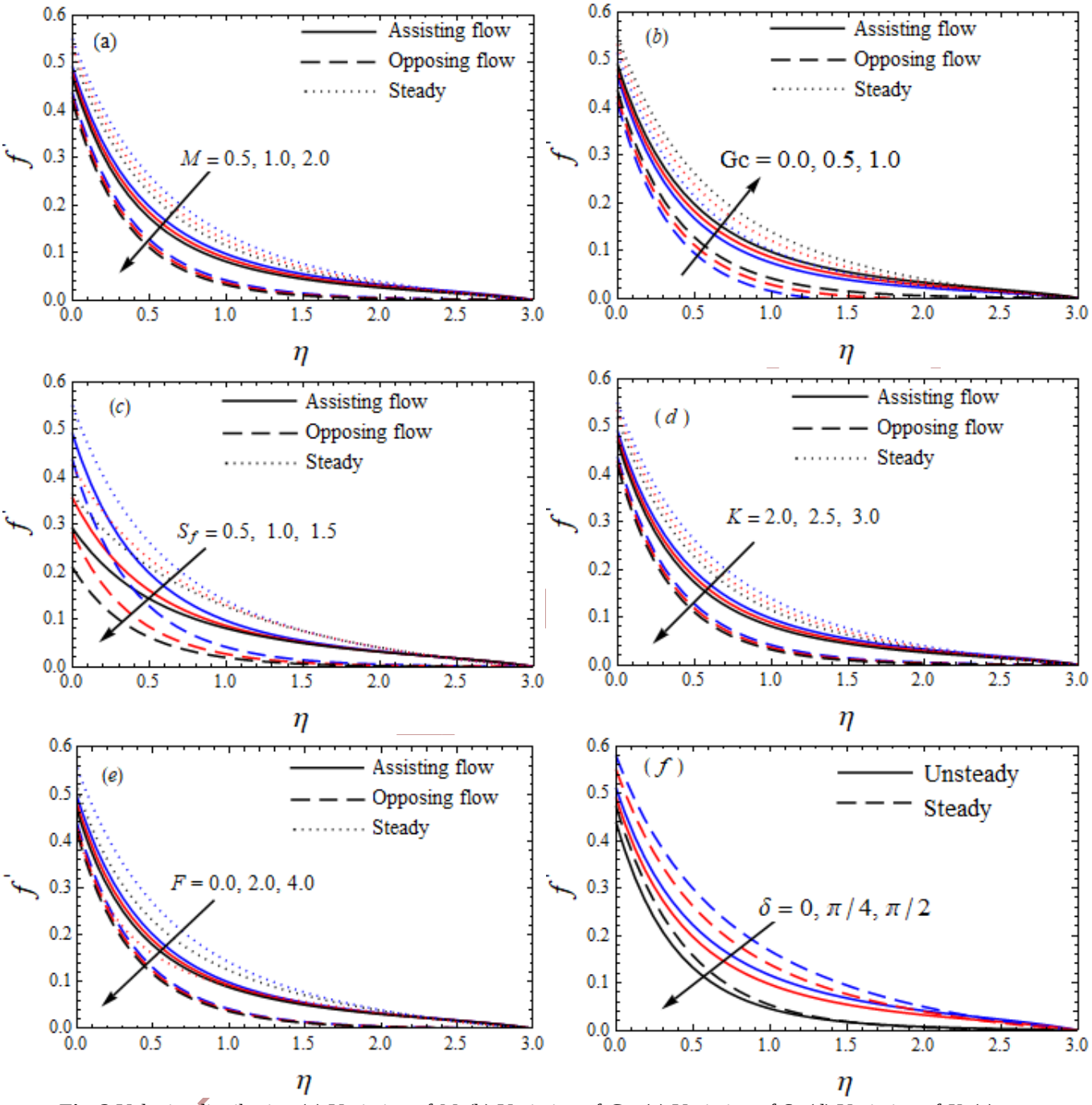

Fig. 2 Velocity distribution (a) Variation of *M*, (b) Variation of *Gc*, (c) Variation of S_f, (d) Variation of *K*, (e) Variation of *F* and (f) Variation of δ.

Fig. 3(d) characterizes the progressions of temperature distribution for various estimation of Prandtl number for opposing, assisting and steady-state cases. Palpably, thermal conductivity attenuations by intensifying the Prandtl number, therefore, temperature profiles attenuations. The changes in the temperature profiles for different estimations of space and temperature dependent uneven energy gain or loss are plotted in Figs. 3(e) and 3(f). It is mentioned that the positive values of space and temperature dependent parameter considered as an energy gain whereas negative values of space and temperature dependent parameter

considered as an energy loss, respectively. Due to this reason, the fluid temperature enhances with uplifting values of space and temperature dependent parameter.

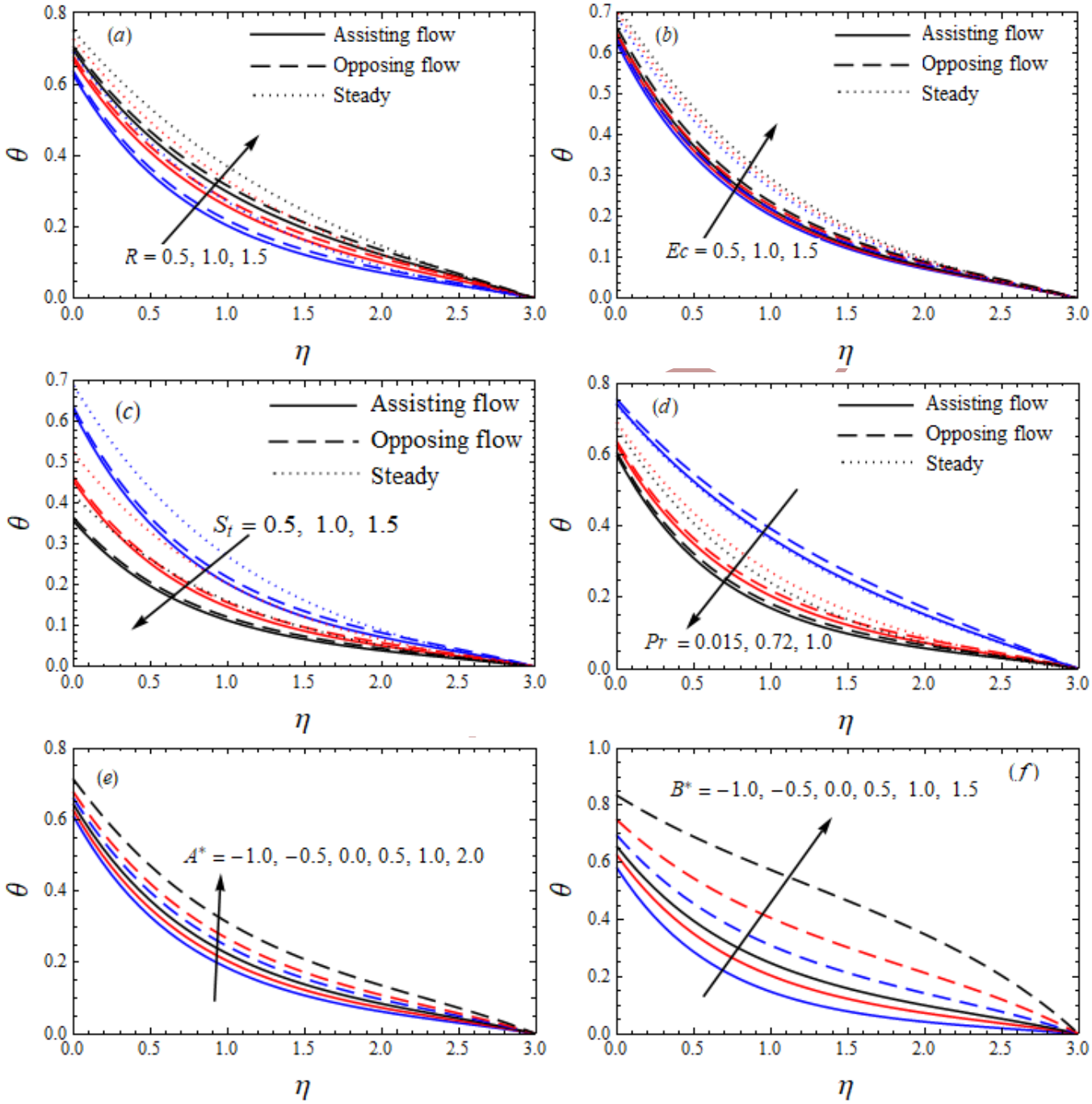

Fig. 3 Temperature distribution (a) Variation of R , (b) Variation of Ec, (c) Variation of S_t, (d) Variation of Pr, (e) Variation of A^* and (f) Variation of B^*.

Figs. 4(a)–(c) portray the impact of concentration on various estimations of solutal slip, Schmidt number, and chemical reaction parameter respectively.

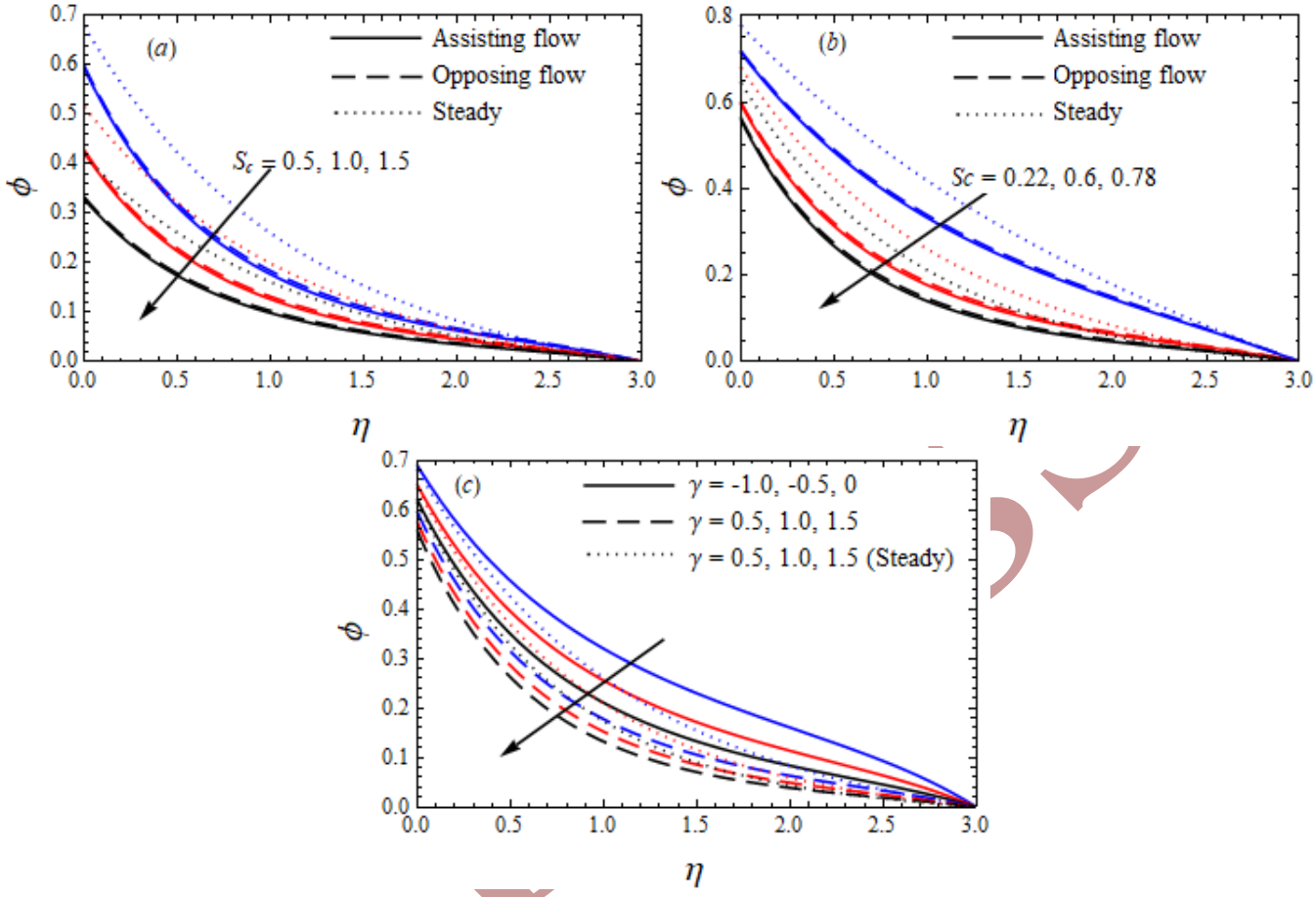

Fig. 4 Concentration distribution (a) Variation of S_c, (b) Variation of *Sc* and (c) Variation of γ .

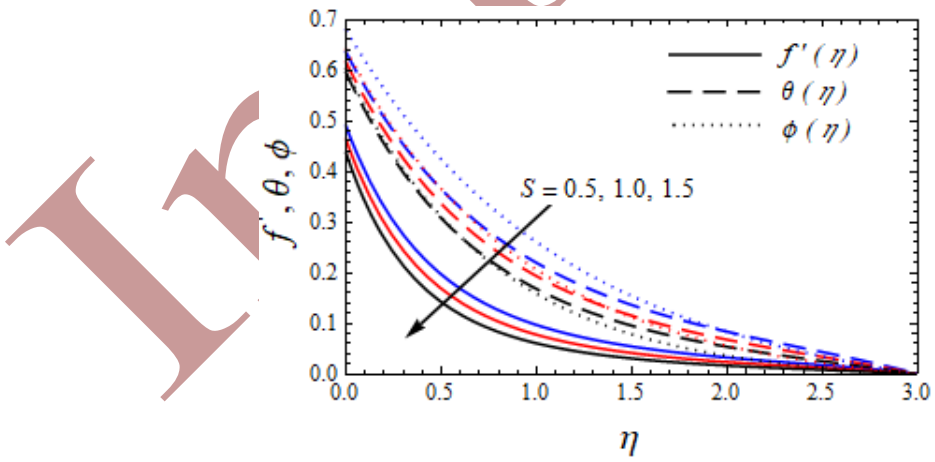

Fig. 5 Velocity, temperature and concentration distributions for variation of S.

Fig. 4(a) is a plotted to exhibits the impact of solutal slip on concentration distribution for cases of opposing, assisting and steady-state. We see from this assume the fixation conveyance of the fluid concentration diminishes as the solutal slip increments. Fig. 4(b) deliberately display the effect of the *Sc* to the concentration distribution. It is notable that the Schmidt number is the ratio between momentum and mass diffusivities. Therefore the higher value of Schmidt number is equivalent to small mass diffusivity. So concentration profile declines. Fig. 4(c)

deliberately display the γ chemical reaction on the concentration profile. It is noteworthy to consider that $(\gamma > 0)$ as a destructive chemical reaction and $(\gamma < 0)$ as a generative chemical reaction, respectively. As a result, both the type of chemical reaction declines the fluid concentration. A variation on fluid velocity, temperature and concentration for the suction parameter are plotted in Fig. 5. It is seems from this figure that the f', θ and ϕ diminish with large values of the suction parameter.

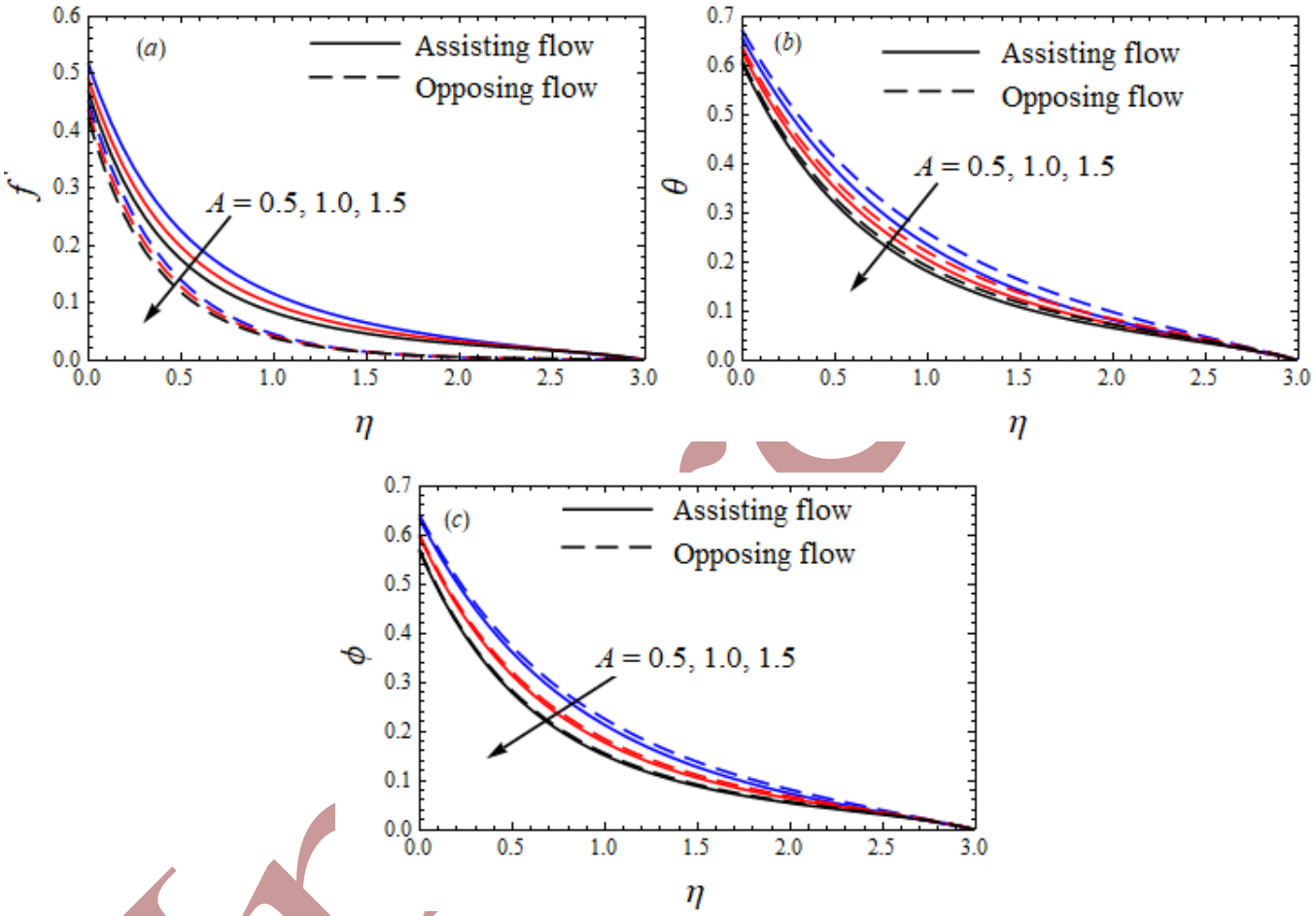

Fig. 6 Variation of A on (a)Velocity (b) temperature and (c) concentration distributions.

Table 2. The variation of $\theta'(0)$ for some reduced cases when $\gamma = 0$, M = *A* = *Da* = *Gr* = *Gc* = *R* = *Ec* = *Sc* = S_f = S_t = 0 = S_c = 0.

Pr	Magyari and Keller [5]	Al-Odat et al. [6]	Pal [7]	Present
0.5	-0.59434	-0.91903	-0.59434	-0.59436
1	-0.95478	-0.57771	-0.95478	-0.95478
3	- 1.86908	-1.81039	-1.86907	-1.86693
5	-2.50014	-2.28864	-2.50013	-2.50014
8	-3.24213	-3.00587	-3.24212	-3.24214
10	-3.66038	-3.18620	-3.66037	-3.66037

Table 3. Changes of $f''(0)$, $-\theta'(0)$ and $-\phi'(0)$ for uplifted values of *Gr*, *Gc*, f_0, *M*, *A*, *K*, *F*, *R*, *Pr*, A^*, B^*, E*c*, *Sc*, γ, $S_f = S_t = S_c = 0.5$, and $\alpha = 45^o$.

Gr	Gc	f_0	*M*	*A*	*K*	*F*	R	Pr	A^*	B^*	*Ec*	Sc	γ	$f''(0)$	$-\theta'(0)$	$-\phi'(0)$
1.0	1.0	0.5	1.0	1.0	2.0	0.5	0.5	0.72	0.5	0.5	0.5	0.6	0.5	-1.001470	0.520708	0.811907
2.0	1.0	0.5	1.0	1.0	2.0	0.5	0.5	0.72	0.5	0.5	0.5	0.6	0.5	-0.930696	0.522769	0.817644
1.0	2.0	0.5	1.0	1.0	2.0	0.5	0.5	0.72	0.5	0.5	0.5	0.6	0.5	-0.953866	0.521791	0.815431
1.0	1.0	1.0	1.0	1.0	2.0	0.5	0.5	0.72	0.5	0.5	0.5	0.6	0.5	-1.055120	0.575950	0.864559
1.0	1.0	0.5	2.0	1.0	2.0	0.5	0.5	0.72	0.5	0.5	0.5	0.6	0.5	-1.048610	0.519833	0.808560
1.0	1.0	0.5	1.0	2.0	2.0	0.5	0.5	0.72	0.5	0.5	0.5	0.6	0.5	-0.509886	0.714610	0.907271
1.0	1.0	0.5	1.0	1.0	3.0	0.5	0.5	0.72	0.5	0.5	0.5	0.6	0.5	-1.048610	0.519833	0.808560
1.0	1.0	0.5	1.0	1.0	2.0	1.0	0.5	0.72	0.5	0.5	0.5	0.6	0.5	-1.010010	0.520691	0.811400
1.0	1.0	0.5	1.0	1.0	2.0	0.5	1.0	0.72	0.5	0.5	0.5	0.6	0.5	-0.996987	0.468829	0.812351
1.0	1.0	0.5	1.0	1.0	2.0	0.5	0.5	1.0	0.5	0.5	0.5	0.6	0.5	-1.010490	0.626750	0.811012
1.0	1.0	0.5	1.0	1.0	2.0	0.5	0.5	0.72	1.0	0.5	0.5	0.6	0.5	-0.997548	0.473498	0.812294
1.0	1.0	0.5	1.0	1.0	2.0	0.5	0.5	0.72	0.5	1.0	0.5	0.6	0.5	-0.989559	0.389880	0.813141
1.0	1.0	0.5	1.0	1.0	2.0	0.5	0.5	0.72	0.5	0.5	1.0	0.6	0.5	-0.999642	0.493358	0.812068
1.0	1.0	0.5	1.0	1.0	2.0	0.5	0.5	0.72	0.5	0.5	0.5	1.0	0.5	-1.011860	0.520266	0.956305
1.0	1.0	0.5	1.0	1.0	2.0	0.5	0.5	0.72	0.5	0.5	0.5	0.6	1.0	-1.004670	0.520565	0.852594

Figs. 6(a)-(c) show the influence of f', θ and ϕ on the unsteadiness parameter. Fig. 6(a) demonstrate the impact of the f' diminishes with the increase of unsteadiness parameter. Unsteadiness parameter changes on θ are displayed in Fig. 6(b) for opposing and assisting flows. We noticed from this figure that the impact of expanding estimations of the unsteadiness parameter is to diminish the θ. Fig. 6(c) is intended to reveal insight into the impact of *A* on the ϕ. It uncovers that the ϕ diminish by uplifted the *A*.

To validate the accuracy of the this model, we compared the numerical results, corresponding to $-\theta'(0)$ and $\theta'(0)$, with the results previously reported in Refs. [2]-[7]. These comparision Tables (1&2) have a good result. The results of shear stress, rate of heat and mass transfer are given in Table 3. $f''(0)$ rises with an large values of *Gr*, *Gc*, *F*, *R*, *Ec* and A^*. $-\theta'(0)$ diminishes with high *M*, *R*, A^*, E, Sc and γ. For large values *Gr*, *S*, *A*, *Sc*, *R*, *Gc*, *Ec*, γ and A^* increases the $-\phi'(0)$.

4. Conclusions

The main goal of this investigation is to exhibits the Darcy-Forchheimer flow of chemically reacting viscous fluid over an inclined exponentially preamble stretching sheet. It is found that velocity, thermal and concentration-related boundary layer thickness declined by uplifted values of a time-dependent parameter. The velocity diminishes with large values of the inclination parameter for both unsteady and steady cases. Temperature increments with large values of the non-uniform heat source; though the turnaround pattern is seen in the case of the sink. The effect of large estimations of Eckert number is to increase the temperature distribution. The outcomes relating to the present investigation demonstrate that due to solutal slip, the concentration diminishes. The skin-friction coefficient is high when the large values of the Grashof number. The local Nusselt number was found to be decreasing as the value of increasing Eckert number.

References

[1] L. J. Crane, "Flow past a stretching plate", *Zeitschrift für Angew. Math. und Phys. ZAMP*, Vol. 21, No. 4, pp. 645–647, (1970).

[2] B. Bidin, and R. Nazar, "Numerical solution of the boundary layer flow over an exponentially stretching sheet with thermal radiation", *Eur. J. Sci. Res.*, Vol. 33, No. 4, pp. 710–717, (2009).

[3] S. Nadeem, S. Zaheer, and T. Fang, "Effects of thermal radiation on the boundary layer flow of a Jeffrey fluid over an exponentially stretching surface", *Numer. Algorithms*, Vol. 57, No. 2, pp. 187–205, (2011).

[4] S. Mukhopadhyay and R. S. R. Gorla, "Effects of partial slip on boundary layer flow past a permeable exponential stretching sheet in presence of thermal radiation", *Heat Mass Transf.*, Vol. 48, No. 10, pp. 1773–1781, (2012).

[5] E. Magyari and B. Keller, "Heat and mass transfer in the boundary layers on an exponentially stretching continuous surface", *J. Phys. D. Appl. Phys.*, Vol. 32, No. 5, pp. 577–585, (1999).

[6] M. Q. Al-Odat, R. A. Damseh, and T. A. Al-Azab, "Thermal boundary layer on an exponentially stretching continous surface in the presence of magnetic field effect", *Int. J. Appl. Mech. Eng.*, Vol. 11, No. 2, pp. 289–299, (2006).

[7] D. Pal, "Mixed convection heat transfer in the boundary layers on an exponentially stretching surface with magnetic field", *Appl. Math. Comput.*, Vol. 217, No. 6, pp. 2356–2369, (2010).

[8] M. Abd El-Aziz, "Viscous dissipation effect on mixed convection flow of a micropolar fluid over an exponentially stretching sheet", *Can. J. Phys.*, Vol. 87, No. 4, pp. 359–368, (2009).

[9] M. Sajid and T. Hayat, "Influence of thermal radiation on the boundary layer flow due to an exponentially stretching sheet", *Int. Commun. Heat Mass Transf.*, Vol. 35, No. 3, pp. 347–356, (2008).

[10] R. Cortell, "Combined effect of viscous dissipation and thermal radiation on fluid flows over a non-linearly stretched permeable wall", *Meccanica*, Vol. 47, No. 3, pp. 769–781, (2012).

[11] P. H. Veena, S. Abel, K. Rajagopal, and V. K. Pravin, "Heat transfer in a visco-elastic fluid past a stretching sheet with viscous dissipation and internal heat generation", *Zeitschrift fur Angew. Math. und Phys.*, Vol. 57, No. 3, pp. 447–463, (2006).

[12] S. R. R. Reddy and P. Bala Anki Reddy, "Bio-mathematical analysis for the stagnation point flow over a non-linear stretching surface with the second order velocity slip and titanium alloy nanoparticle", *Front. Heat Mass Transf.*, Vol. 10, No. 13, pp. 1–11, (2018).

[13] S. Gupta, D. Kumar, and J. Singh, "MHD mixed convective stagnation point flow and heat transfer of an incompressible nanofluid over an inclined stretching sheet with chemical reaction and radiation", *Int. J. Heat Mass Transf.*, Vol. 118, pp. 378–387, (2018).

[14] A. Saadatmandi and Z. Sanatkar, "Collocation method based on rational Legendre functions for solving the magneto-hydrodynamic flow over a nonlinear stretching sheet", *Appl. Math. Comput.*, Vol. 323, pp. 193–203, (2018).

[15] P. Kumar, K. Tanmoy, and C. Kalidas, "Framing the Cattaneo – Christov heat flux Phenomena on CNT- based Maxwell

Nanofluid along stretching sheet with multiple slips", *Arab. J. Sci. Eng.*, Vol. 43, No. 3, pp. 1177–1188, (2018).

[16] P. B. A. Reddy and N. B. Reddy, "Thermal radiation effects on hydro-magnetic flow due to an exponentially stretching sheet", *Int. J. Appl. Math. Comput.*, Vol. 3, No. 4, pp. 300–306, (2011).

[17] M. M. Bhatti, M. A. Abbas, and M. M. Rashidi, "A robust numerical method for solving stagnation point flow over a permeable shrinking sheet under the influence of MHD", *Appl. Math. Comput.*, Vol. 316, pp. 381–389, (2018).

[19] S. R. R. Reddy, P. Bala Anki Reddy, and S. Suneetha, "Magnetohydrodynamic flow of blood in a permeable inclined stretching surface with viscous dissipation, non-uniform heat source/sink and chemical reaction", *Front. Heat Mass Transf.*, Vol. 10, No. 22, pp. 1–10, (2018).

[20] K. Vajravelu, K. V. Prasad, and C. O. Ng, "Unsteady convective boundary layer flow of a viscous fluid at a vertical surface with variable fluid properties", *Nonlinear Anal. Real World Appl.*, Vol. 14, No. 1, pp. 455–464, (2013).

[21] P. B. A. Reddy and N. B. Reddy, "Finite difference analysis of radiation effects on unsteady MHD flow of a chemically reacting fluid with time-dependent suction", *Int. J. Appl. Math Mech.*, Vol. 7, No. 9, pp. 96–105, (2011).

[22] A. J. Chamkha, A. M. Aly, and M. A. Mansour, "Similarity solution for unsteady heat and mass transfer from a stretching surface embedded in a porous medium with suction / injection and chemical reaction effects", *Chem. Eng. Commun.*, Vol. 197, No. 6, pp. 846–858, (2010).

[23] D. Pal and N. Roy, "Lie group transformation on MHD double-diffusion convection of a Casson nanofluid over a vertical stretching / shrinking surface with thermal radiation", *Int. J. Appl. Comput. Math.*, Vol. 13, No. 4, pp. 1–23, (2018).

[24] N. Bachok, A. Ishak, and I. Pop, "Unsteady boundary-layer flow and heat transfer of a nanofluid over a permeable stretching/shrinking sheet", *Int. J. Heat Mass Transf.*, Vol. 55, No. 7–8, pp. 2102–2109, (2012).

[25] D. Pal, "Combined effects of non-uniform heat source/sink and thermal radiation on heat transfer over an unsteady stretching permeable surface", *Commun. Nonlinear Sci. Numer. Simul.*, Vol. 16, No. 4, pp. 1890–1904, (2011).

[26] J. C. Misra and A. Sinha, "Effect of thermal radiation on MHD flow of blood and heat transfer in a permeable capillary in stretching motion", *Heat Mass Transf.*, Vol. 49, No. 5, pp. 617–628, (2013).

[27] S. Srinivas, P. B. A. Reddy, and B. S. R. V. Prasad, "Non-Darcian unsteady flow of a micropolar fluid over a porous stretching sheet with thermal radiation and chemical reaction", *Heat Transf. Res.*, Vol. 44, No. 2, pp. 172–187, (2015).

[28] Yan Zhang, Min Zhang, and Shujuan Qi, "Heat and mass transfer in a thin liquid film over an unsteady stretching surface in the presence of thermo solutal capillarity and variable magnetic field", *Mathematical Problems in Engineering*, Vol. 2016, pp. 8521580, (2016).

[29] M. Hatami, Kh. Hosseinzadeh, G. Domairry, M. T. Behnamfar, "Numerical study of MHD two-phase Couette flow analysis for fluid-particle suspension between moving parallel plates", *Journal of the Taiwan Institute of Chemical*

Engineers, Vol. 45, No. 5, 2238-2245, (2014).

[30] S. S. Ghadikolaei, Kh. Hosseinzadeh, and D. D. Ganji, "Analysis of unsteady MHD Eyring-Powell squeezing flow in stretching channel with considering thermal radiation and Joule heating effect using AGM", *Case Studies in Thermal Engineering*, Vol. 10 pp. 579-594, (2017).

[31] K. Das, "Slip flow and convective heat transfer of nanofluids over a permeable stretching surface", *Comput. Fluids* Vol. **64**, pp. 34-42, (2012).

[32] M. Swati, "Slip effects on MHD boundary layer flow over an exponentially stretching sheet with suction/blowing and thermal radiation", *Ain Shams Engineering J.* Vol. **4**, pp. 485-491, (2013).

[33] A.J. Chamka, A.M. Aly, and M.A. Mansour, "Similarity solution for unsteady Heat and Mass transfer from a stretching surface embedded in a porous medium with suction/injection and chemical reaction effects", *Chem. Eng. Comm.* Vol. **197**, pp. 846-858, (2010).

[34] J.C. Misra, and A. Sinha, "Effect of thermal radiation on MHD flow of blood and heat transfer in a permeable capillary in stretching motion", *Heat Mass Transfer*, Vol. **49**, pp. 617-628, (2013).